

3D Printing Technique for a New Efficient Production Method of mm-wave Antennas

A.Vorobyov¹, I. Montesinos-Ortego², S. Unterhofer¹, B. Galocha Iragüen³, M. Sierra-Castañer³

¹ CSEM: Centre Suisse d'Electronique et de Microtechnique SA, Neuchatel, Switzerland, oleksandr.vorobyov@csem.ch

² TTI Antennas Department, Santander, Spain, imontesinos@ttinorte.es*

³ Universidad Politécnica de Madrid. ETSI Telecomunicación. Information Processing and Telecommunications Centre. Madrid, Spain, manuel.sierra@upm.es

Abstract—This paper presents the 3D printed metallic planar slotted antenna array operating at 94GHz. A reliable and cost-effective additive manufacturing method has been optimized for high printing resolutions. The prototyped antennas were characterized, and performance was compared with the theoretical estimation.

Index Terms—antennas, 3D printing, mm-wave, radar, measurements.

I. INTRODUCTION

An mm-wave waveguide-based radar is one of the parts of the complex flight vision system in civil aircraft to assist pilots to land under any visibility circumstances. The EU-funded 3DGUIDE project aims to demonstrate a cost-effective production method for high-precision mm-wave waveguide antennas with 3D printing. This is a promising process to manufacture antennas with complex 3D shapes used in any mm-wave communication or sensing systems and particularly in Enhanced Flight Vision Systems (EFVS) to considerably reduce their production cost with the potential to also decrease radar weight.

There are many traditional methods of manufacturing waveguides and WG-based RF components (e.g., filters). Diffusion bonding and split block solutions are the most technologically advanced compared to traditional methods. However, they are very expensive and time-consuming to prototype.

3D printing in metal enables the manufacturing of functional parts through an innovative approach. A Laser Powder Bed Fusion (L-PBF) technology opens new horizons allowing the fabrication of parts, that are limited or cannot be produced in any conventional way. Production of the mm-wave components based on L-PBF additive manufacturing, optimized for high resolution (<0.5% down to less than 10 μ m), with freedom of shaping allowing for an increased level of integration, with a large variety of materials including aeronautics-proven materials.

During the previous EuCAP conference, the design and measurements of a linear slot array were presented [1]. In that paper, the design was tested, and a first prototype was performed to validate the fabrication method. In this paper, three different planar array antenna prototypes working at 94 GHz. have been built and measured. The selected manufacturing process, (L-PBF) has been optimized for high printing resolutions at CSEM [2][3][4][5]. The electrical

parameters of the antenna array have been measured and they are presented in this document.

The paper is organized as follows: Target antenna specification is provided in Section II. Section III describes the antenna design methodology. Section IV describes chosen AM-based production technology and the realized 3D-printed antennas. Antenna characterization and results discussion is addressed in Section V. The conclusion is provided in Section VI.

II. ANTENNA SPECIFICATIONS

To validate the objective of the 3DGUIDE project, a planar antenna array working at 94 GHz is designed and fabricated. The electrical specifications of this design are presented in TABLE I.

TABLE I. ANTENNA SPECIFICATIONS

Parameter	Target Value
WG type	WR10
Centre frequency	94GHz (EFVS standard)
Bandwidth	2.5GHz
Return Loss	> 15dB (Target > 18dB)
Antenna type	WG slotted linear array
Number of slots	64
Antenna Directivity @ 94GHz	23.5dBi
Antenna beamwidth 3dB	E - plane $\approx 7.1^\circ$ H - plane $\approx 9.6^\circ$
Polarization	Linear
XPD at boresight	> 50dB
Beam scan	Broadside fixed beam

Three different prototypes have been fabricated to analyze the most appropriate fabrication method.

III. ANTENNA DESIGN METHODOLOGY

Prior to the design of the complete bidimensional array, the linear grouping of slots was designed using the MoM-FMP technique. It combines the method of moments (MoM) with the Equivalent Circuit Model, and Forward Matching Procedure (FMP) to construct linear arrays of slots,

independently of the operation frequency, in a systematic way, fast, and accurate [6][7]. A database is generated by several evaluations (MoM) of the single slot in different configurations depending on structural properties such as length, offset (distance from the waveguide axis), width, tilting angle, etc.. The next step is to compose an equivalent electrical network (Π or T circuit) for each case of the database, creating a repository of candidates, which are appropriately connected, using FMP. This connection considers impedance properties aiming to keep the input matched at the selected frequency while a specific amplitude taper is generated along the array. Once the configuration that satisfies the best-given specs is found, MoM-FMP returns the architectural properties of the slots within the array, such as position, offset, length and the length of the last short-circuited section.

A. Bidimensional array

The single vector array is then eight times repeated along the transverse direction with respect to the array axis to compose the bidimensional grouping of 64 radiators (8-by-8 array). The mutual coupling between homologous slots of contiguous linear arrays is very strong and an iterative optimization process is carried out to mitigate its unwanted effects in the electrical performance of the array.

B. Feeding network

Considering the manufacturing techniques to be used in the project, the feeding network follows a corporate architecture based on H-plane power dividers/combiners with a mechanical constraint of 0.2mm wall thickness. They also include chamfered bends with no radii according to the inherent mechanical properties of additive manufacturing.

To facilitate the accommodation of the demonstrator to the anechoic chamber positioner, the waveguide flange (antenna input) has been placed opposite to the radiating aperture. To do so, a 90° E-plane ben with a capacitive iris has been included in the model.

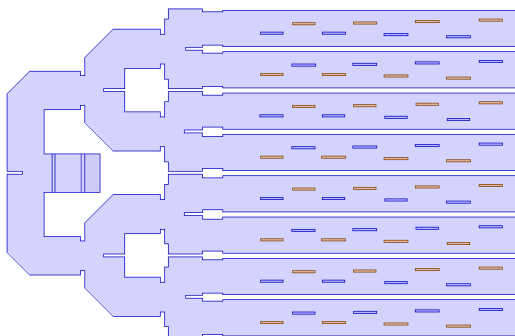


Fig. 1. HFSS model of the whole antenna

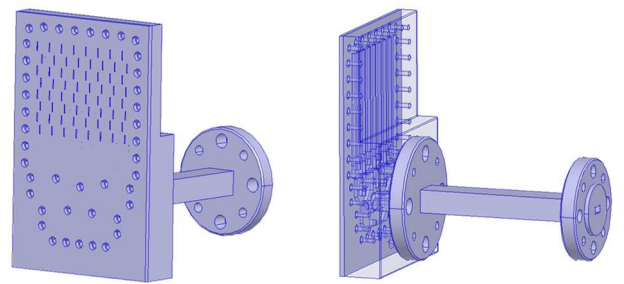
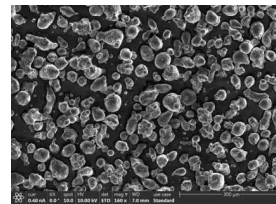


Fig. 2. Picture of the antenna and the interface to the positioner.

IV. FABRICATION PROCESS

Laser Powder Bed Fusion (L-PBF) 3D printing is an Additive Manufacturing process for metal materials that have been used for antenna prototyping. Building parts layer by layer by depositing material according to the digital 3D design data, this process allows complex 3D design prototyping.

Material choice was investigated to achieve a lower level of RF losses, which was finally applied to an Aluminum alloy (Fig.3) allowing thin features fabrication ($160\mu\text{m}\pm 15$) with a surface roughness of ~ 7 to $10\mu\text{m}$ after printing (As-Built). Further surface treatment (chemical polishing and metal plating) allows for bringing the surface roughness below 4 to $6\mu\text{m}$.



Powder size distribution:
 $D_{10} = 24.5\mu\text{m}$; $D_{90} = 61.5\mu\text{m}$
 Flowability:
 Hausner ratio 1.21 (-)
 Chemical composition (wt%):
 87.4% Al. 12.0% Si. 0.6%

Fig. 3. AlSi12 specification.

The full chain process optimization (Fig. 4) consists of three complementary parts: Feedstock materials, the LPBF process and post-processing.

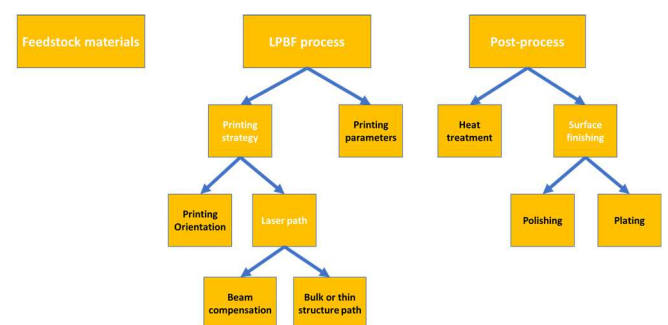


Fig. 4. Full chain 3D printing process.

An adaptation of the printing orientation, of the laser path and the chemical polishing, needs to be developed for any components printed. Printing parameters (for bulk structure), heat treatment and electroless silver plating are just slightly dependent on the design.

Printing orientation, as a part of the printing strategy, is an extremely important factor that was used to achieve small as-built roughness on all the inner surfaces (Fig.5).

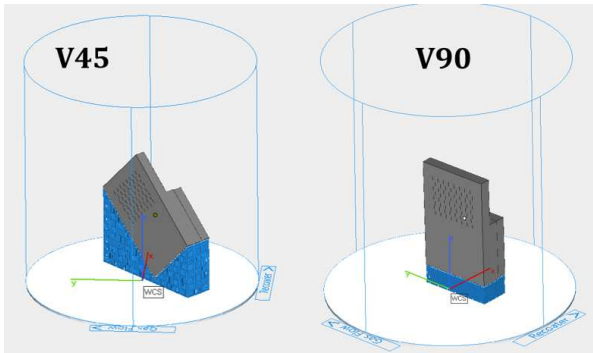
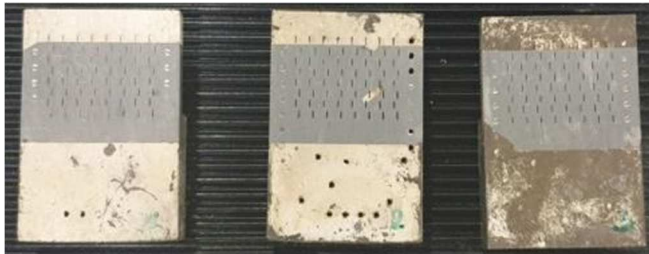


Fig. 5. Example of antenna array printing orientations.

Three different prototypes of the antenna presented in Section 3 have been manufactured at CSEM (Fig. 6). The three prototypes are different from each other concerning printing orientation, beam compensation and laser polishing for up-skin surfaces.



- Prototype 1 Printing orientation V45
Beam compensation of 35um
- Prototype 2 Printing orientation V90
Beam compensation of 50um
No up-skin laser polishing
- Prototype 3 Printing orientation V90
Beam compensation of 50um
Up-skin laser polishing

Fig. 6. Picture of the fabricated antennas: from left to right Prototype_1, Prototype_2 and Prototype_3.

Prototypes 2 and 3 are printed at V90 orientation, with surfaces at 0°. They're both up-skin and down-skin surfaces are low in quality concerning roughness and have less precision in dimensions. An electrical discharge machining (EDM) can be used to increase the roughness and dimension precision of the down-skin surfaces, but for the current prototypes, this post-process has not been performed. Concerning up-skin surfaces, laser polishing has been tested. This technic consists of consecutive laser melting during the printing process, only when the last layer (up-skin surfaces) is achieved. For prototype 3, the laser track passed 6 times consecutively to polish the surface.

Post-processes are kept the same for the three samples, which are:

- Deep machining on the joining surface: at least 1 mm
- Heat treatment: 350°C, 1h, air
- Chemical polishing: Keller, 4:20 min, r.t.
- Mechanical polishing: 0.5 mm wall thickness reduction
- Sandblasting on the joining surface: perpendicularly, 5 s
- Electroless silver plating: 30 min

A. Fabrication Timing details

The prototyping time depends on the number of antennas created simultaneously. As an example: 10 samples of prototyping take around 27h. The distribution of the time is provided in the table below. However, we can proceed at least twice faster when the process is optimised.

TABLE II. ANTENNA PROTOTYPING TIMES

Process	Time [h]
3D printing	15
Heat treatment	1
Mechanical post-treatment	5
Chemical polishing	4
Silver plating	3
Total time	27
Time for single antenna	2h45

V. MEASUREMENTS

The prototypes were tested in the facilities of the Universidad Politécnica de Madrid Antenna Measurements facilities [8]. The measured parameters were reflection coefficient, radiation pattern, gain, directivity and losses.

A. Reflection coefficient

The reflection coefficient is shown in Fig. 7 for the three prototypes.

The main conclusions for these measurements are:

- The fabrication process has an inherent strong impact in the reflection coefficient.
- Among the existing results it is more than evident that Antenna 2 exhibits better matching properties.
- Global performance is acceptable, whichever the selected fabrication methodology is selected.

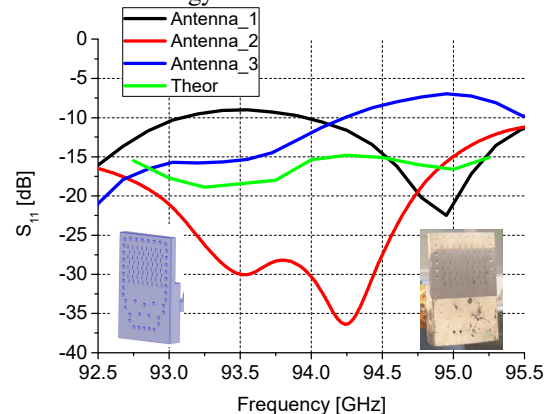


Fig. 7. Measured Reflection Coefficient of the prototyped antennas.

B. Radiation Pattern

Also, the radiation pattern for the different prototypes has been measured in the frequency band. In Fig. 8, the radiation pattern at the central frequency for the first prototype is shown. Similar results were found for the other two prototypes.

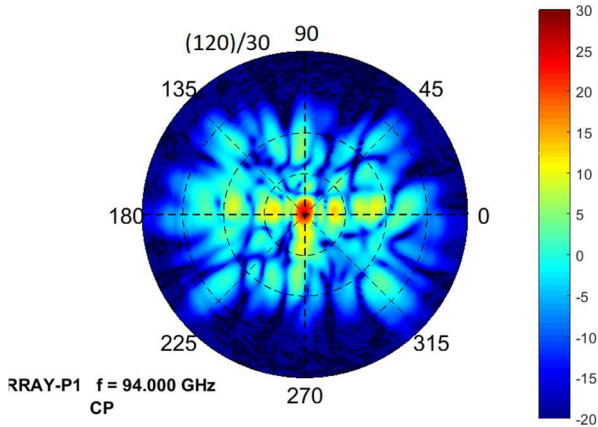


Fig. 8. 3D Radiation pattern for Prototype_1 at 94 GHz.

The main conclusions for the radiation pattern measurement are:

- The radiation patterns are equivalent to the theoretical ones.
- Some de-pointing in the vertical plane appears for the Antennas 1 and 2.
- The cross-polar radiation is good enough for all three prototypes.

C. Gain, directivity and losses

Gain, directivity, and losses are also measured for the three prototypes. Fig. 9 shows the broadside directivity and the ohmic losses. The results for the directivity are good, getting the 23.5 dBi in the central frequency for Antennas 1 and 3, while for Antenna_2 there is a frequency shift to the upper frequencies of the band due to the fabrication process. In the case of the ohmic losses, the best antenna is Antenna 2 with 0.5 dB of losses, and the worst is Antenna 1 with 1.5 dB in the central frequency. In any case, the results for the three fabrication processes are encouraging.

In order to analyze this frequency shift, the amplitude and phase for each slot of the Antenna_2 have been analyzed using the combination of the methods proposed in [9] and [10]. It is observed that the amplitude is higher in the right part of the antenna while the phase presents a linear slope. This is the reason for the beam-pointing error and the shift in the frequency response.

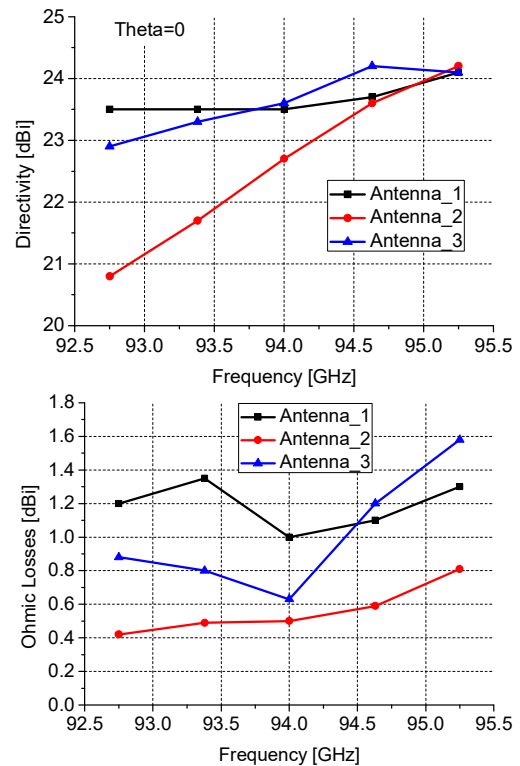
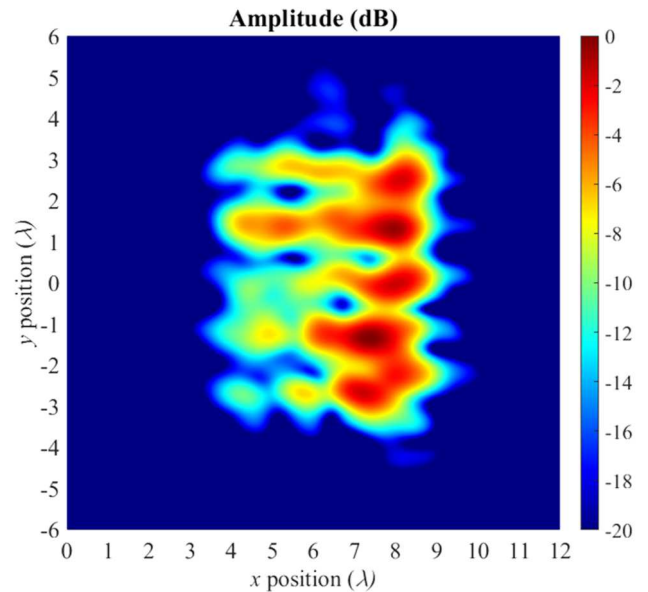


Fig. 9. Directivity and ohmic losses for the three prototypes in the frequency band.



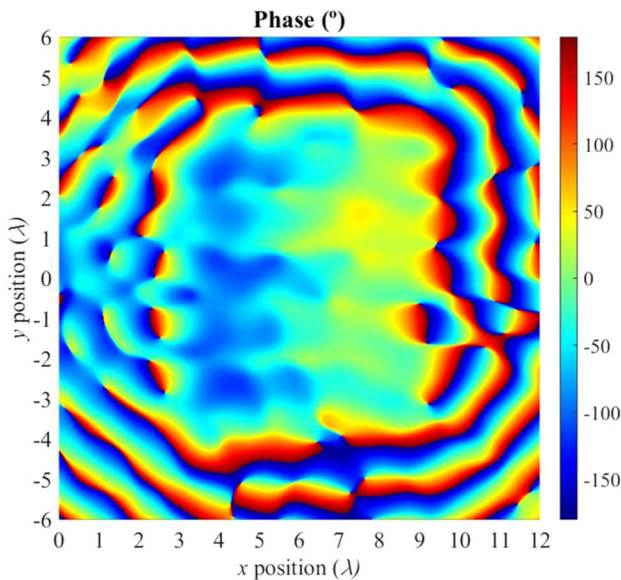


Fig. 10. Amplitude and phase of the currents on each slot for the second prototype.

VI. CONCLUSIONS

The design freedom provided by L-PBF technology has already shown many advantages in micro-wave component manufacturing, such as weight reduction and assembly simplification.

Three prototypes have been fabricated and measured. The results are very promising, although they could be improved in future fabrication steps finetuning:

- The directivity of Antenna 1 is very good, although is a bit more lossy and there are also some problems of impedance matching.
- The directivity of Antenna 2 is centred in the upper part of the frequency band. The losses in this case are very small and it is very well matched. It presents a tilt in the vertical plane that can be corrected in a second phase.
- The Antenna 3 is the best in terms of directivity, gain, losses, and radiation pattern. However, it presents a mismatch in the upper frequencies of the band.

The obtained results show 3D printing potential in manufacturing antennas in this frequency band (94 GHz) with complex 3D shapes (e.g. waveguide-based components) with reduced assembly steps and lower costs.

This suggests that this manufacturing technique is suitable in terms of both mechanical and electrical characteristics.

ACKNOWLEDGMENT

The research leading to these results has received funding from the CleanSky Programme under grant agreement no. 886696 and was carried out in the frame of 3DGUIDE project

(Feasibility demonstration of 3D printing for a new efficient production method of mm-wave waveguide antenna).

REFERENCES

- [1] I. Montesinos-Ortego, M. García-Peña, B. Galocha-Iragüen and M. Sierra-Castañer, "Manufacturing and Testing of a 94GHz Linear Slot Array Designed by the MoM-FMP Technique," 2022 16th European Conference on Antennas and Propagation (EuCAP), 2022, pp. 1-4, doi: 10.23919/EuCAP53622.2022.9769077.
- [2] M. D'Auria, W. J. Otter, J. Hazell, B. T. W. Gillatt, C. Long-Collins, N. M. Ridler and a. S. Lucyszyn, "3-D Printed Metal-Pipe Rectangular Waveguides," *IEEE Transactions on Components, Packaging and Manufacturing Technology*, Vols. vol. 5, no. 9, p. pp. 1339–1349, Sept 2015.
- [3] E. Decrossas, T. Reck, C. Lee, C. Jung-Kubiak, I. Mehdi and G. Chattopadhyay, "Evaluation of 3D printing technology for corrugated horn antenna manufacturing," in *IEEE International Symposium on Electromagnetic Compatibility (EMC)*, 2016.
- [4] J. Shen, M. W. Aiken, M. Abbasi and D. P. Parekh, "Rapid Prototyping of Low Loss 3D Printed Waveguides for Millimeter-Wave Applications," in *IEEE MTT-S International Microwave Symposium (IMS)*, 2017.
- [5] S. Unterhofer, O. Sereda, O. Vorobyov, M. Dadrás, "Additive manufacturing of smart waveguide: comparison between three alloys, Bronze, Al-Si and Scalmalloy", European Congress and Exhibition on Advanced Materials and Processes 2021
- [6] I. Montesinos-Ortego, M. Zhang, M. Sierra-Perez, J. Hirokawa and M. Ando, "Systematic Design Methodology for One-Dimensional Compound Slot-Arrays Combining Method of Moments, Equivalent Circuit Model and Forward Matching Procedure," in *IEEE Transactions on Antennas and Propagation*, vol. 61, no. 1, pp. 453-458, Jan. 2013, doi: 10.1109/TAP.2012.2220108.
- [7] I. Montesinos-Ortego, M. Zhang, M. Sierra-Pérez, J. Hirokawa and M. Ando, "Versatility of MoM-FMP technique for designing linear arrays of slots on rectangular waveguide," 2012 International Symposium on Antennas and Propagation (ISAP), 2012, pp. 138-141.
- [8] LEHA-UPM facilities. <https://www.gr.ssr.upm.es/index.php/en/leha/about-us>
- [9] F. Cano, M. Sierra-Castañer, S. Burgos and J. L. Besada, "Applications of sources reconstruction techniques: Theory and practical results," *Proceedings of the Fourth European Conference on Antennas and Propagation*, 2010, pp. 1-5.
- [10] M. Sano, M. Sierra-Castañer, T. Salmerón-Ruiz, J. Hirokawa and M. Ando, "Reconstruction of the Field Distribution on Slot Array Antennas Using the Gerchberg-Papoulis Algorithm," in *IEEE Transactions on Antennas and Propagation*, vol. 63, no. 8, pp. 3441-3451, Aug. 2015, doi: 10.1109/TAP.2015.2434391.